Inhibition of Hsp90 with Synthetic Macrolactones: Synthesis and Structural and Biological Evaluation of Ring and Conformational Analogs of Radicicol

Nicolas Proisy,[1] Swee Y. Sharp,[2] Kathy Boxall,[2]
Stephen Connelly,[3] S. Mark Roe,[4]
Chrisostomos Prodromou,[4] Alexandra M.Z. Slawin,[5]
Laurence H. Pearl,[4] Paul Workman,[2]
and Christopher J. Moody[1,*]
[1] School of Chemistry
University of Nottingham
University Park
Nottingham, NG7 2RD
United Kingdom
[2] Cancer Research UK Centre for Cancer Therapeutics
The Institute of Cancer Research
Haddow Laboratories
15 Cotswold Road
Sutton
Surrey, SM2 5NG
United Kingdom
[3] Department of Chemistry
University of Exeter
Exeter, EX4 4QD
United Kingdom
[4] Section of Structural Biology
The Institute of Cancer Research
Chester Beatty Laboratories
237 Fulham Road
London, SW3 6JB
United Kingdom
[5] School of Chemistry
University of St. Andrews
Fife
Scotland, KY16 9ST
United Kingdom

Summary

A series of benzo-macrolactones of varying ring size and conformation has been prepared by chemical synthesis and evaluated by structural and biological techniques. Thus, 12- to 16-membered lactones were obtained by concise routes, involving ring-closing metathesis as a key step. In enzyme assays, the 13-, 15-, and 16-membered analogs are good inhibitors, suggesting that they can adopt the required conformation to fit in the ATP-binding site. This was confirmed by cocrystallization of 13-, 14-, and 15-membered lactones with the N-terminal domain of yeast Hsp90, showing that they bind similarly to the "natural" 14-membered radicicol. The most active compounds in the ATPase assays also showed the greatest growth-inhibitory potency in HCT116 human colon cancer cells and the established molecular signature of Hsp90 inhibition, i.e., depletion of client proteins with upregulation of Hsp70.

*Correspondence: c.j.moody@nottingham.ac.uk

Introduction

Heat shock protein 90 (Hsp90) is one of the most abundant proteins in eukaryotic cells and is an ATP-dependent chaperone that plays a central role in regulating the stabilization, activation, and degradation of a range of proteins [1–3]. These "clients" include a number of key proteins involved in cell cycle regulation and signal transduction (see http://www.picard.ch/downloads/Hsp90interactors.pdf). Furthermore, among Hsp90's client proteins are a number of known overexpressed or mutant oncogenic proteins such as C-RAF, B-RAF, ERBB2, AKT, telomerase, and p53, many of which are associated with the six hallmarks of cancer [4, 5]. Consequently, Hsp90 has become an attractive target for novel cancer therapeutic agents, since its inhibition will disrupt multiple cancer-causing pathways simultaneously [4, 6–10]. Recently, it has been suggested that targeting Hsp90 may also halt neurodegeneration [11].

The Hsp90 proteins possess a conserved ATP-binding pocket in the N-terminal domain [12, 13], and it is disruption of ATP binding (and subsequent hydrolysis) that leads to proteasomal degradation of client proteins [14]. Most inhibitors of Hsp90 bind to the N-terminal ATP site [15, 16], although the naturally occurring antibiotic novobiocin is known to bind at the C terminus and is therefore also of interest [17–19]. Known inhibitors include the natural products radicicol, 1, and geldanamycin, 2, both of which have been cocrystallized with the yeast protein; the protein-bound structures of 1 and 2 were determined by X-ray crystallography [15]. The binding of both radicicol, 1, and geldanamycin, 2, to the protein has also been studied in solution by NMR spectroscopy [20]. A derivative of geldanamycin, 17-allylamino-17-desmethoxygeldanamycin (17-AAG), 3, is the first-in-class inhibitor of Hsp90 to enter the clinic and is now in phase II trial [21, 22]. Several unnatural (designed), synthetic inhibitors are ATP mimics and are based on the purine framework, as exemplified by PU3, 4a, and PU24FC1, 4b, and by the closely related arylsulfanyl compound PU-H58, 5 [23–28]. However, other families of inhibitors are now emerging, in particular the 3-(2,4-dihydroxyphenyl)pyrazoles [29], as in CCT018159, 6a [30, 31], G3130, 6b [32], and VER-49009, 6c [33, 34], while members of the most recently discovered family contain the 1-aryl-2-naphthol moiety as in compound 7 [35] (Figure 1).

Of these inhibitors (Figure 1), radicicol, 1 (also known as monorden), originally isolated from the fungus *Monocillium nordinii* [36], and subsequently from both *Nectria radicicola* [37] and from the plant-associated fungus *Chaetomium chiversii* [38], is the most potent in vitro [39], although it has little or no activity in vivo [40, 41]. This is presumably a result of its instability, particularly toward conjugate addition to the dienone moiety, although its oxime derivative did possess some in vivo activity [42]. The natural product itself has attracted the interest of synthetic chemists and has been the subject of three total syntheses by the groups of Lett [43–46], Danishefky [47], and Winssinger [48]. In a search for further

4a PU3; X = Y= H, R = C4H9
4b PU24FCl; X = F, Y = Cl, R = (CH2)3C≡CH

1 radicicol

2 geldanamycin; R = OMe
3 17-AAG; R = NHCH2CH=CH2

PU-H58 **5**

6a CCT018159; R = Et, R^1 = Me, R^2 = 2,3-dihydrobenzodioxin-6-yl
6b G3130; R = Et, R^1 = H, R^2 = imidazol-4-yl
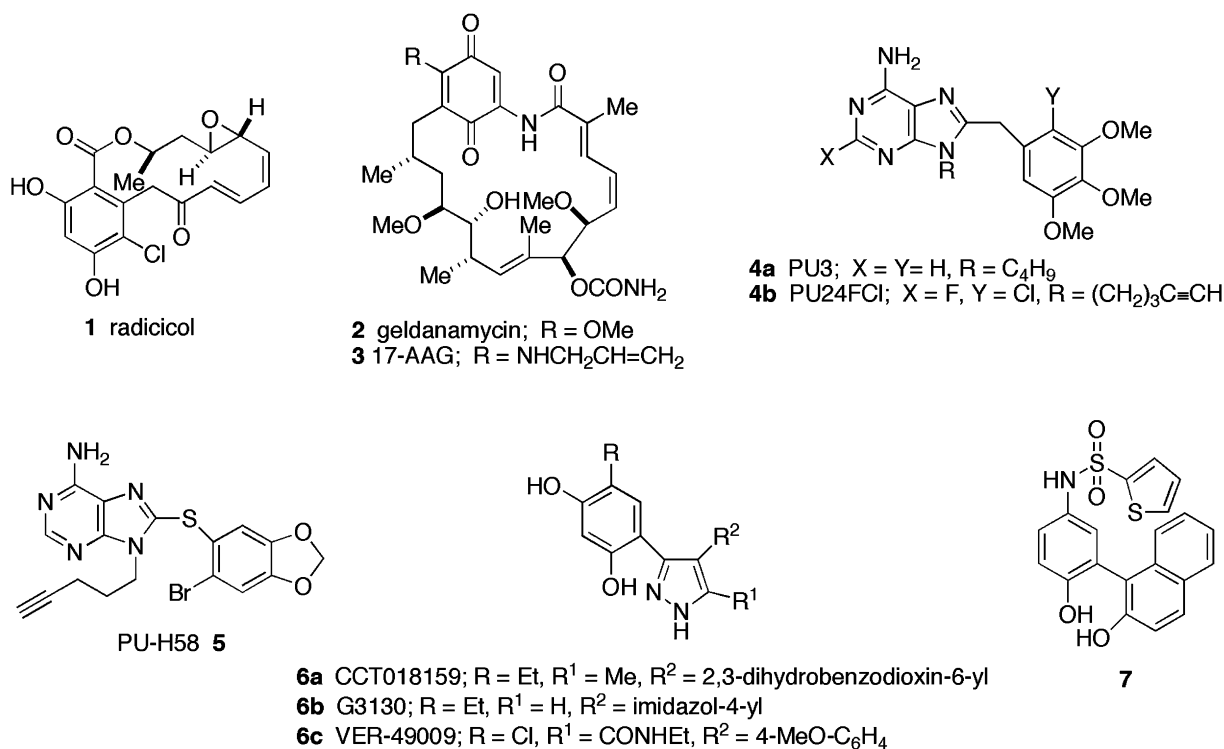**6c** VER-49009; R = Cl, R^1 = CONHEt, R^2 = 4-MeO-C6H4

7

Figure 1. Structures of Hsp90 Inhibitors

biologically active analogs, Danishefsky and coworkers have developed a novel series of inhibitors based on cycloproparadicicol [49–51]. These molecules, obtained by quite lengthy chemical synthesis, show promising activity and demonstrate that modified synthetic analogs of radicicol do have potential as anticancer compounds. Further work in this area [52–57], including a very recent study that attempts to identify the key features of the 14-membered ring of radicicol that are necessary for biological activity [38], has been reported of late.

The aim of the present study is the design and chemical synthesis of a series of radicicol analogs of different ring size, and hence conformation; the characterization of their binding to Hsp90 by protein crystallography and molecular modeling; and their biological evaluation. The results of this integrated chemistry/biology approach are described herein.

Results and Discussion

The starting point for our work was a reconsideration of the detailed structure of radicicol, **1**, bound in the ATP pocket in the N-terminal domain of yeast Hsp90 [15], particularly in light of the more recent biological data on radicicol analogs [49–51]. The yeast and human enzymes exhibit 88% similarity (70% identity) between their N-terminal domains. Within 5 Å of bound ADP, there are only two differences between the yeast and human proteins, namely, Ala38 (human Ser52) and Leu173 (human Val186), which are approximately 4 and 5 Å, respectively, from the exocyclic N6 of the adenine ring of ADP. Consequently, all of the key interactions with ADP, ATP, and various Hsp90 inhibitors such as geladamycin and radicicol are essentially the same. The crystal

structure of radicicol, **1**, bound to yeast Hsp90 (Figure 2A) shows that the antibiotic adopts a folded conformation and that the key hydrogen-bonding interactions involve the salicylate ester and phenolic groups with water molecules. Most importantly, the carboxylate side chain of Asp79, the main chain amide group of Gly83, and the hydroxyl side chain of Thr171 interact with radicicol via the same tightly bound water molecule. Another interaction occurs between the main chain carbonyl of Leu34 and radicicol, via another water molecule. Although the structure clearly shows the involvement of the epoxide oxygen in hydrogen bonding to the ε-amino side chain of Lys44, the relatively minimal 2-fold loss of in vitro activity in the corresponding cyclopropane suggests that this interaction, although useful, is not essential [49].

Therefore, we decided on a series of compounds that not only lacked this epoxide, but also the sensitive dienone fragment. We also decided to simplify the structures further by removing the remaining stereocenter by investigating compounds lacking the methyl group α to the macrolactone oxygen. However, our major objective was the synthesis and evaluation of smaller and larger ring sizes, since the conformation of the 14-membered macrolactone is thought to have an important influence on binding to Hsp90 [55], and hence the biological activity of radicicol analogs. It is the structural and biological evaluation of different ring sizes resulting in varying conformations of the radicicol analogs that distinguishes our work from that previously published.

Chemical Synthesis
The synthetic routes for the novel radicicol analogs start with the known benzoic acid derivative, **8**, an
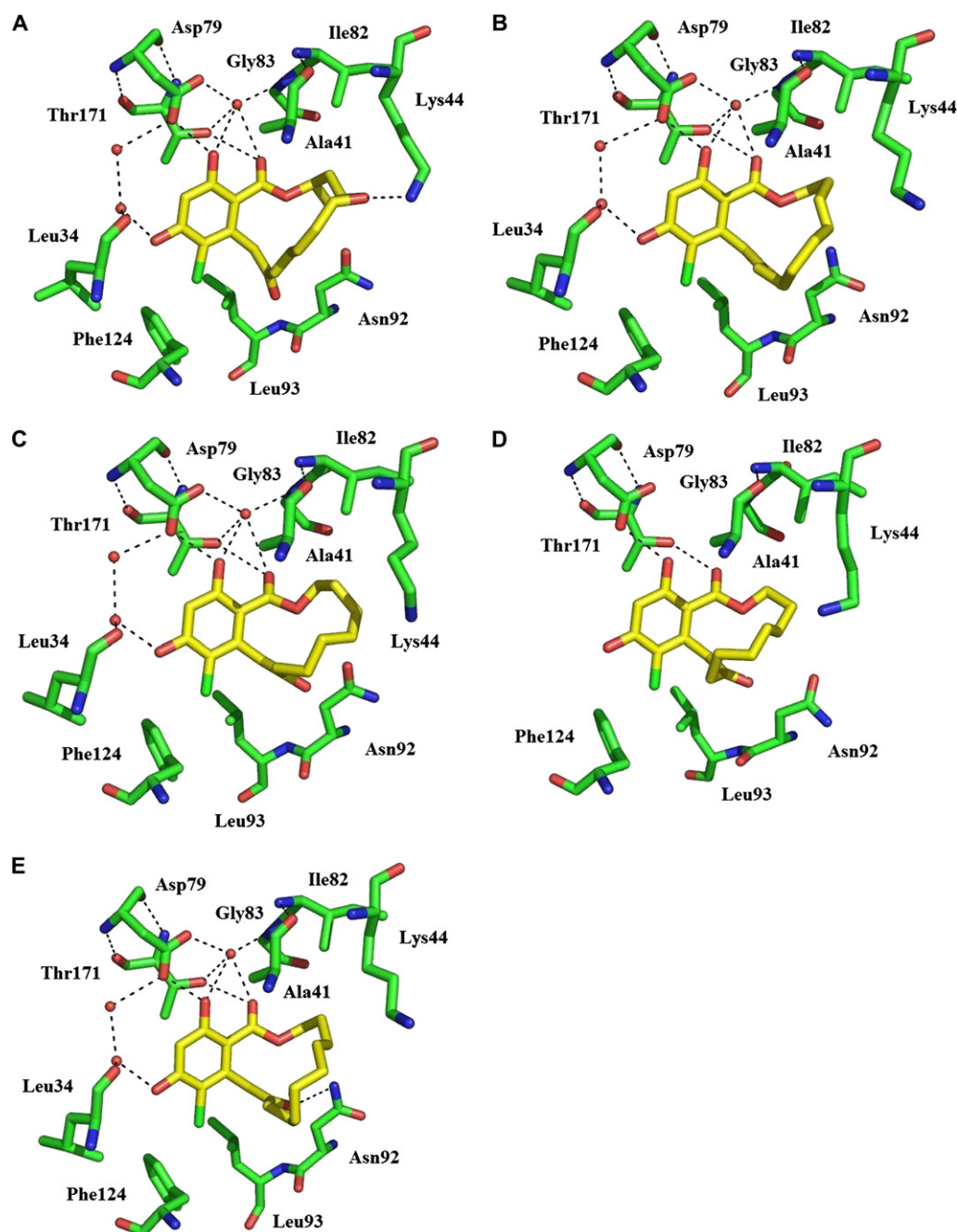
Figure 2. Binding Interactions of Macrolactone Inhibitors with Yeast Hsp90

(A–E) In all cases, the hydrogen-bonded interactions in the ATP-binding site are represented as broken lines. (A) Radicicol, **1** (data taken from [15]; data are available at PDB ID: 1BGQ). (B) 14-membered lactone, **15a** (PDB ID: 2CGF). (C) 13-membered lactone, **15f** *cis* (PDB ID: 2IWS). (D) 13-membered lactone, **15f** *trans* (PDB ID: 2IWU). (E) 15-membered lactone, **15h** (PDB ID: 2IWX).

intermediate in Danishefsky and coworkers' first-generation synthesis of radicicol [47]. Mitsunobu esterification with 3-butenol gave benzoate, **9a**, in which the chloride was displaced by the anion derived from 2-(5-hexenyl)-1,3-dithiane, **10a**, to give **11a**. Protection of the phenol as its *tert*-butyldimethylsilyl (TBDMS) ether, **12a**, was followed by the ring-closing metathesis (RCM) reaction to generate the macrocycle, a tactic commonly used in related syntheses [47, 48, 50, 57, 58]. Thus, use of the Grubbs second-generation catalyst, benzylidene(1,3-

bis[2,4,6-trimethylphenyl]-2-imidazolidinylidene)dichloro-(tricyclohexylphosphine)ruthenium, gave the 14-membered ring **13a**. Deprotection of the thioketal and silyl ethers by using bis(trifluoroacetoxy)iodobenzene [59] and tetra-*n*-butylammonium fluoride (TBAF), respectively, gave resorcinol, **14a**, chlorination of which gave the desired chloride, **15a** (Figure 3). The sequence was repeated by using racemic, (S)-4-penten-2-ol, and (R)-4-penten-2-ol to give the corresponding racemic, (R)-14-membered, and (S)-14-membered rings, **15b**, **15c**,
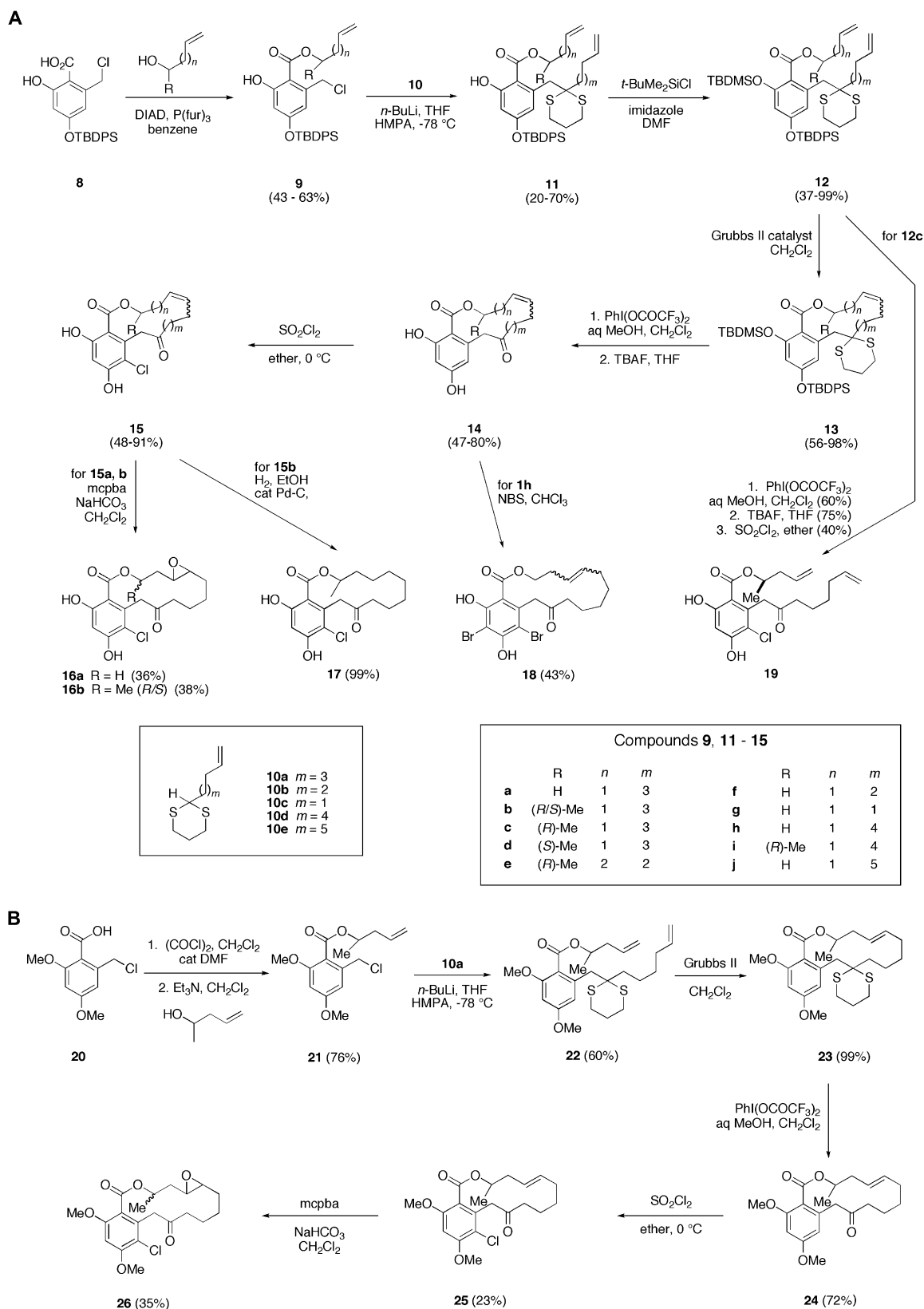
A

8

9
(43 - 63%)

11
(20-70%)

12
(37-99%)

15
(48-91%)

14
(47-80%)

13
(56-98%)

16a R = H (36%)
16b R = Me (R/S) (38%)

17 (99%)

18 (43%)

19

		10a	m = 3
		10b	m = 2
		10c	m = 1
		10d	m = 4
		10e	m = 5

Compounds 9, 11 - 15

	R	n	m		R	n	m
a	H	1	3	f	H	1	2
b	(R/S)-Me	1	3	g	H	1	1
c	(R)-Me	1	3	h	H	1	4
d	(S)-Me	1	3	i	(R)-Me	1	4
e	(R)-Me	2	2	j	H	1	5

B

20

21 (76%)

22 (60%)

23 (99%)

26 (35%)

25 (23%)

24 (72%)

Figure 3. Synthesis of Radicicol Analogs

(A) Synthesis of resorcinol-type derivatives; DIAD = di-isopropyl azodicarboxylate.
(B) Synthesis of resorcinol dimethyl ethers.
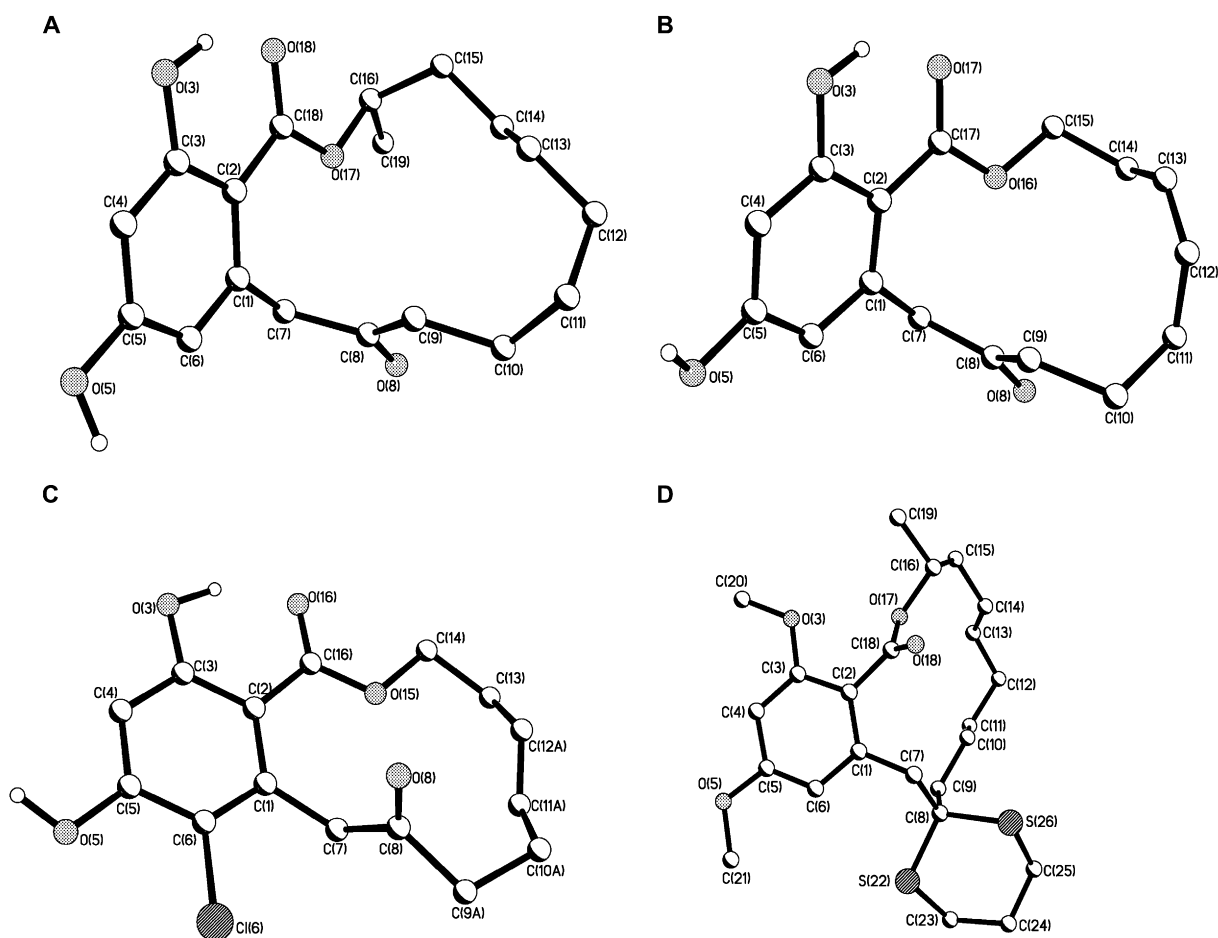
Figure 4. X-Ray Crystal Structures, Showing Crystallographic Numbering, of Macrolactones

(A) 14-membered ring **14b**.
(B) 13-membered ring **14f**.
(C) 12-membered ring **15g**.
(D) 14-membered ring **23**.

and **15d**, respectively, as shown in Figure 3. The stereochemistry of the alkene formed in the RCM reaction was established as *trans* (*E*) by an X-ray crystallographic analysis of the macrocycle **14b** (Figure 4A) that shows the intramolecular hydrogen bond of salicylate ester. The position of chlorination was established by using NMR spectroscopy.

Our synthetic route is extremely versatile, and via changes in the chain length of the starting alcohol or in the 2-alkenyl-1,3-dithiane, **10**, one can readily access a wide range of compounds. Hence it is possible to investigate binding of synthetic analogs of different conformations, such as the 14-membered ring with the double bond in a different position (**15e**), both the *cis* and *trans* 13-membered rings (**15f**), the 12-membered ring (**15g**), the 15-membered rings (**15h** and **15i**), and the 16-membered ring (**15j**), to the ATP-binding site of Hsp90. The preparation of these analogs is summarized in Figure 3A. Wherever possible, the alkene geometry was confirmed by X-ray crystallography as shown for the *cis* 13-membered ring intermediate, **14f**, and the *trans* 12-membered ring, **15g** (Figures 4B and 4C), or by NMR spectroscopy (*trans J* = 12–15 Hz; *cis J* = ∼7 Hz).

Alkenes **15a** and **15b** were converted into the corresponding epoxides, **16a** and **16b**, by reaction with 3-chloroperoxybenzoic acid, and **15b** was also reduced to the corresponding alkane, **17**. The 15-membered ring **14h** was also brominated (NBS), rather than chlorinated, although the product was the dibromide, **18**, as opposed to the expected monobromide. The flexible open-chain diene, compound **19**, was prepared from **12c** as shown in Figure 3A. Finally, the dimethoxy compounds **25** and **26** were also prepared for comparison purposes from the known benzoic acid, **20** [47]; the *trans* alkene was again confirmed by X-ray crystallographic analysis of the dithiane intermediate, **23** (Figures 3B and 4D).

Protein Crystallography
The macrocycle, **15a**, was cocrystallized with the N-terminal domain of yeast Hsp90, and the structure of the resulting complex was solved by molecular replacement. The structure (Figure 2B) shows that the compound binds in a similar way to radicicol, and that it retains the key water molecules in the H-bonding network. However, the direct interaction with the ε-amino side
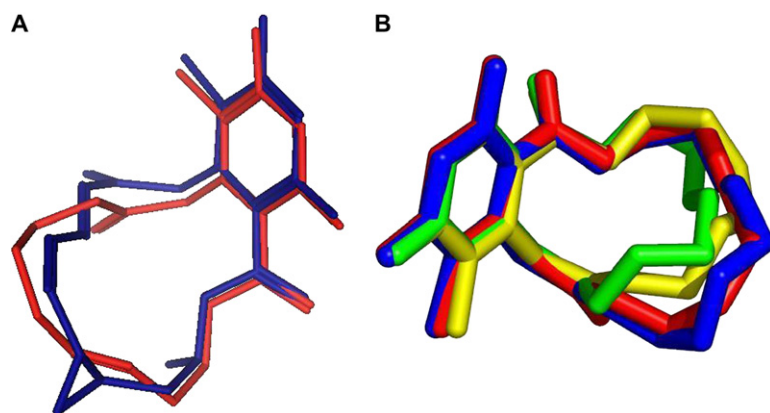
Figure 5. Molecular Modeling

(A) Overlaid structures of protein-bound conformations of radicicol (blue) and synthetic macrolactone, **15a** (red).

(B) Overlaid structures of protein-bound conformations of synthetic macrolactones: 14-membered lactone, **15a** (red), 13-membered lactone, **15f** *cis* (yellow), 13-membered lactone, **15f** *trans* (green), and 15-membered lactone, **15h** (blue).

chain of Lys44 is replaced by hydrophobic interactions with **15a** due to the loss of the epoxide oxygen. A common set of hydrophobic interactions between the protein and the inhibitors, **15a** and **1**, are also seen (Asn37, Asp40, Ile82, Met84, Phe124 and Leu173), and Ala41 is also involved in a hydrophobic interaction with **15a**. Likewise, both *cis* and *trans* 13-membered rings, **15f** *cis* and **15f** *trans*, respectively, and the 15-membered ring **15h** were cocrystallized with the N-terminal domain of yeast Hsp90. The structures are shown in Figures 2C–2E, and they essentially bind in the same way as **15a**. However, there is an additional hydrogen-bond interaction between the side chain of Asn92 and the O5 oxygen of **15h**. The structures for **15f** *cis* and **15h**, with drastically different ring sizes and conformations, are accommodated within the hydrophobic surface that is the same as that which interacts with radicicol, **1**, and there are no significant alterations in the ATP-binding site that result from interactions with **15f** *cis* and **15h**. The data collected for **15f** *trans* were substantially weaker than those for **15f** *cis* (average I/σI, 7.4; cf. 17.3). Consequently, the refinement was not as straightforward, leading to higher R and R_{free} values for this structure, even though the density for the inhibitor was clear. For this reason also, only the most tightly bound water molecules were located in the difference maps.

With X-ray data available, it was possible to conduct modeling experiments to compare the bound conformation of radicicol and the simplified analog, **15a**. The structures of both **15a** and radicicol within Hsp90 were energy minimized by using the Monte Carlo method (MOE software). By combination of the resulting structures, it was observed that the protein fragments overlay almost perfectly. The protein was then masked to simultaneously show the conformation of **15a** and radicicol, which exhibited a high degree of similarity. The results are shown in Figure 5A. Likewise, it was possible to overlay the protein-bound conformations of the14-membered lactone, **15a**, with the *cis* and *trans* 13-membered rings, **15f**, and the15-membered lactone, **15h**, as shown in Figure 5B. While the 14- and 15-membered rings adopt similar conformations, the two 13-membered rings are different, both from each other and from the two higher ring sizes, highlighting the ability of the ATP site to accommodate the varying ring sizes and conformations presented by these analogs. Isothermal titration calorimetry confirmed that **15a**, **15f** *cis*, **15f**
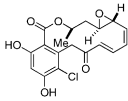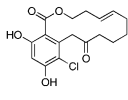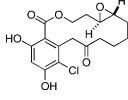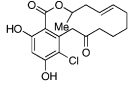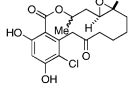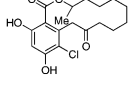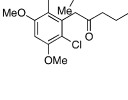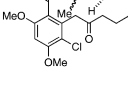
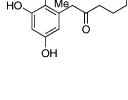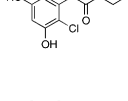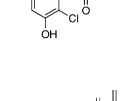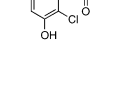*trans*, and **15h** bound with similar affinity to intact yeast Hsp90 (K_d = 0.39, 0.44, 1.2, and 0.21 μM, respectively; results not shown), though with a higher K_d than radicicol (K_d = 0.007 μM).

Biological Evaluation

The novel compounds were evaluated in the malachite green assay for Hsp90 ATPase activity [60], and also by using a fluorescence polarization (FP) assay [33, 61]. As shown previously, the more sensitive FP assay gives IC_{50} values about 5–10 times lower than the ATPase assay [33, 61]. The results are shown in Table 1. It is immediately apparent that many of these "stripped down" 14-membered ring analogs of radicicol retain considerable biological activity; the simplest analog, **15a**, and its racemic methyl homolog, **15b**, are only 3- to 8-fold less potent than the structurally more complex natural product. As expected, the "natural" (R)-methyl compound, **15c**, is more potent than the racemate, **15b**, and it is only 2-fold less potent than radicicol in the FP assay. The "unnatural" (S)-isomer, **15d**, is less potent than the racemate. The epoxides **16a** and **16b** have similar potency to their alkene precursors, and while the deschloro compound **14c** retains some activity, the dibromide, **18**, is less potent. Both the alkane, **17**, and the flexible open-chain diene, **19**, are ~20-fold less active than their cyclic alkene counterparts, while compound **15e** with the double bond in a different position is significantly less active, demonstrating the effect of the double bond on the conformation of the macrocycle. Not surprisingly, removal of the H-bonding capacity of the phenolic groups, as in the dimethoxy compounds **25** and **26**, results in almost complete loss of activity.
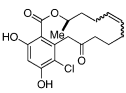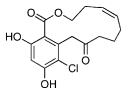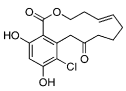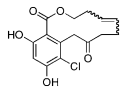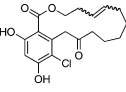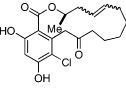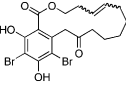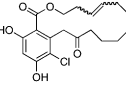
Our versatile synthetic chemistry also provided access to 12-, 13-, 15-, and 16-membered ring analogs for comparison with the "natural" 14-membered ring compounds. Of these, the *cis* and *trans* 13-membered rings, **15f**, were slightly less active than their 14-membered homolog, and despite their differing conformations, they have similar activity to each other (~0.5 μM in the FP assay); the 12-membered ring **15g** is less potent still (~4 μM). While the 15-membered rings **15h** and **15i** (0.1–0.2 μM) essentially retain the same activity as its 14-membered analog, **15a** (0.11 μM), the 16-membered ring **15j** (>0.2 μM) is slightly less potent. Unfortunately, although the 14-membered ring **15a** could be

Table 1. Inhibition of Yeast Hsp90 by Macrolactones

Entry	Compound	Structure	FP Assay, IC$_{50}$ (μM)	ATPase Assay, IC$_{50}$ (μM)	SRB Assay, IC$_{50}$ (μM)
1	1		0.047, 0.03	0.2	0.025, 0.068
2	15a		0.12, 0.10	<1, 1.3	3.2, 2.9
3	16a		0.19, 0.31	2.1, 2.5	5.5, 6.4
4	15b		0.16, 0.31	1, 1.5	12, 17
5	16b		0.31, 0.25	1.9, 2.2	1.8, 2.6
6	17		1.29, 3.23	23, 34	33, 66
7	25		38.2, 24.0	>100, >100	16, 28
8	26		58.4	>100, >100	42, 88
9	14c		0.54, 0.50	4, 3.2	23, 22
10	15c		0.10, 0.10	<1, 1	4.7, 7.2
11	15d		3.4, 5.4	>10	76, 68
12	19		2.1, 2.9	16, 27	29, 27

(Continued)

Table 1. *Continued*

Entry	Compound	Structure	FP Assay, IC$_{50}$ (μM)	ATPase Assay, IC$_{50}$ (μM)	SRB Assay, IC$_{50}$ (μM)
13	**15e**		1.9, 1.9	10	35, 33
14	**15f** *cis*		0.50, 0.85	2.4	22, 14
15	**15f** *trans*		0.59, 1.0	3.5	10, 8.6
16	**15g**		4.18, 3.8	13	48, 60
17	**15h**		0.16, 0.10	0.76	6, 15
18	**15i**		0.22, 0.16	4.9, 4.3	20
19	**18**		2.63, 1.1	—	40, 64
20	**15j**		0.24, 0.87	—	38, 48

obtained as a pure (*E*)-alkene isomer, both the 15- and 16-membered rings contained a small amount (5%–15%) of the (*Z*)-alkene isomer.

The most potent compounds in the FP and ATPase assays also show the greatest growth-inhibitory potency in the HCT116 human colon cancer cell line, as measured by the SRB assay. Compounds showing the greatest cell growth-inhibitory activity were those that were most potent against the Hsp90 enzyme, including **15a**, **16a**, **16b**, and **15c**. It should be pointed out, however, that the difference between potency in the FP assay and that in cells is much greater for the potent synthetic compounds (e.g., **15b** or **16b**) than for radicicol. Also, when comparing **15b** and **16b**, it is clear that the difference in cellular potency between these compounds correlates only poorly with their activity in the FP assay. It is reasonable to speculate that these discrepancies may be due to differences in cell uptake. It is possible that the natural product radicicol benefits from a cellular uptake mechanism that cannot be accessed by the current synthetic inhibitors. To confirm

that growth inhibition was due to the intended mechanism, we assessed compounds **15a**, **15c**, and **15h** for their effect on the established molecular signature of Hsp90 inhibition [3]. Figure 6 shows depletion of client proteins C-RAF, ERBB2, and CDK4, together with upregulation of Hsp70, thus confirming that the new, to our knowledge, analogs were acting as Hsp90 inhibitors in the cell. No effect was seen with the essentially inactive analog, **26**.

Significance

Structural analysis of the Hsp90-radicicol complex has facilitated the design of a series of analogs of the 14-membered ring macrocyclic lactone natural product, and the different ring sizes and conformations have allowed us to investigate the ability of the ATP-binding site to accept such radicicol analogs. These novel analogs retain potent binding and inhibitory activity against the ATPase activity of Hsp90. They are structurally much less complex than radicicol and, hence,
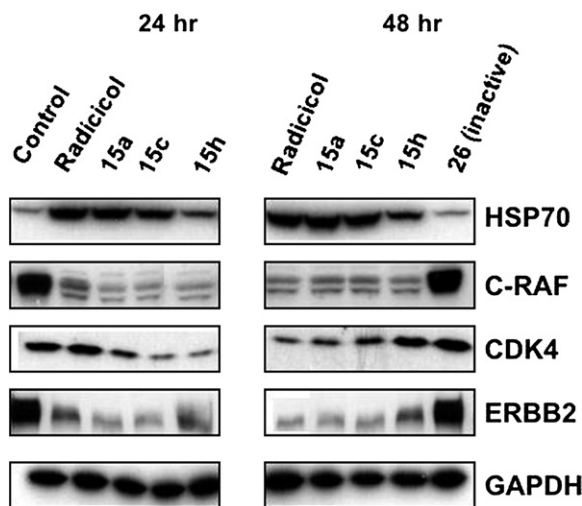
Figure 6. Western Blot Showing Depletion of Client Proteins C-RAF, ERBB2, and CDK4, with Upregulation of Hsp70, upon Treatment with Radicicol and Macrolactones

GAPDH was used as a loading control. HCT116 cells treated with $5 \times IC_{50}$ of compound. The dimethoxy analog, **26**, which is essentially inactive ($IC_{50} > 50$ μM), was tested at 65 μM.

are readily accessible by chemical synthesis. Of particular interest is the high activity of "unnatural" ring sizes such as the 15-membered ring homolog. Protein crystallography has shown that the ATP site unexpectedly can readily accommodate analogs of differing ring sizes and conformations. Biological studies demonstrated that growth-inhibitory activity against human colon cancer cells was due to Hsp90 inhibition by confirming client protein depletion and Hsp70 upregulation.

Experimental Procedures

Chemistry
Characterization data for final products are described below.

(R)-2,4-Dihydroxy-7-methyl-7,8,11,12,13,14-hexahydro-6-oxa-16H-benzocyclotetradecene-5,15-dione 14c
mp 172°C −174°C; $[\alpha]_D^{23} - 98.0$ (c 1.00, CHCl$_3$); (Found: C, 67.5; H, 7.0. C$_{18}$H$_{22}$O$_5$ requires C, 67.9; H, 7.0%); (Found: M$^+$, 318.1467. C$_{18}$H$_{22}$O$_5$ requires 318.1454); ν_{max} (KBr)/cm^{-1} 3391, 2943, 2923, 1688, 1654; δ_H (300 MHz; CDCl$_3$) 11.96 (1 H, s, OH), 7.38 (1 H, s, OH), 6.37 (1 H, d, J 1.9, ArH), 6.16 (1 H, d, J 1.9, ArH), 5.53–5.30 (3 H, m, C$\underline{H}$=C$\underline{H}$, OC$\underline{H}$Me), 4.00 (2 H, AB, J 16.6, ArC$\underline{H}_2$), 2.64–1.40 (10 H, m, 5 × CH$_2$), 1.40 (3 H, d, J 6.4, Me); δ_C (75 MHz; CDCl$_3$) 210.8, 170.6, 165.7, 160.2, 139.0, 135.1 (CH), 124.6 (CH), 112.2 (CH), 105.5, 102.9 (CH), 72.9 (CH), 49.8 (CH$_2$), 40.8 (CH$_2$), 37.7 (CH$_2$), 32.5 (CH$_2$), 25.1 (CH$_2$), 22.2 (CH$_2$), 19.0 (Me); m/z (FI) 318 (M$^+$, 10%), 133 (13), 108 (35).

(E)-1-Chloro-2,4-dihydroxy-7,8,11,12,13,14-hexahydro-6-oxa-16H-benzocyclotetradecene-5,15-dione 15a
mp 168°C −169°C; (Found: C, 60,0; H, 5.6. C$_{17}$H$_{19}$ClO$_5$ requires C, 60.3; H, 5.65%); (Found: M$^+$, 338.0916. C$_{17}$H$_{19}^{35}$ClO$_5$ requires 338.0921); ν_{max} (KBr)/cm^{-1} 3241, 2927, 2863, 1699, 1654, 1240; δ_H (300 MHz; CDCl$_3$) 11.81 (1 H, s, OH), 6.58 (1 H, s, ArH), 6.50 (1 H, s, OH), 5.56–5.37 (2 H, m, C$\underline{H}$=C$\underline{H}$), 4.43 (2 H, t, J 5.4, OC$\underline{H}_2$), 4.28 (2 H, s, ArC$\underline{H}_2$), 2.58 (2 H, t, J 6.4, C$\underline{H}_2$CO), 2.40–2.40 (2 H, m, CH$_2$), 2.12–2.08 (2 H, m, CH$_2$), 1.74–1.66 (2 H, m, CH$_2$), 1.59–1.53 (2 H, m, CH$_2$); δ_C (75 MHz; CDCl$_3$) 207.0, 171.0, 163.7, 156.4, 136.1 (C) 134.0 (CH), 126.1 (CH), 114.7, 107.0, 103.5 (CH), 65.5 (CH$_2$), 46.7 (CH$_2$), 40.9 (CH$_2$), 32.2 (CH$_2$), 31.5 (CH$_2$), 25.5 (CH$_2$), 22.0 (CH$_2$); m/z (FI) 340/338 (M$^+$, 41/100%), 304 (5).

(R)-1-Chloro-2,4-dihydroxy-7-methyl-7,8,11,12,13,14-hexahydro-6-oxa-16H-benzocyclotetradecene-5,15-dione 15c
mp 130°C −132°C; $[\alpha]_D^{23} - 22.0$ (c 1.00, CHCl$_3$); (Found: M$^+$, 352.1073. C$_{18}$H$_{21}^{35}$ClO$_5$ requires 352.1078); ν_{max} (KBr)/cm^{-1} 3320, 2934, 2856, 1704, 1651, 737; δ_H (300 MHz; CDCl$_3$) 11.75 (1 H, s, OH), 6.61 (1 H, s, ArH), 6.21 (1 H, s, OH), 5.47–5.33 (3 H, m, C$\underline{H}$=C$\underline{H}$, OC$\underline{H}$Me), 4.25 (2 H, AB, J 17.7, ArC$\underline{H}_2$), 2.62–1.41 (10 H, m, 5 × CH$_2$), 1.39 (3 H, d, J 6.4, Me); δ_C (75 MHz; CDCl$_3$) 206.7, 170.0, 163.5, 156.1, 136.1, 135.2 (CH), 124.3 (CH), 114.6, 107.6, 103.5 (CH), 73.1 (CH), 46.7 (CH$_2$), 41.0 (CH$_2$), 37.6 (CH$_2$), 32.4 (CH$_2$), 25.2 (CH$_2$), 22.0 (CH$_2$), 18.8 (Me); m/z (EI) 354/352 (M$^+$, 6/16%), 183 (100).

(S)-1-Chloro-2,4-dihydroxy-7-methyl-7,8,11,12,13,14-hexahydro-6-oxa-16H-benzocyclotetradecene-5,15-dione 15d
mp 131°C −133°C; $[\alpha]_D^{23} + 16.0$ (c 1.00, CHCl$_3$); (Found: MH$^+$, 353.1159. C$_{18}$H$_{21}^{35}$ClO + H requires 353.1156); ν_{max} (KBr)/cm^{-1} 3320, 2934, 2856, 1704, 1651, 737; δ_H (300 MHz; CDCl$_3$) 11.75 (1 H, s, OH), 6.61 (1 H, s, ArH), 6.21 (1 H, s, OH), 5.47–5.33 (3 H, m, C$\underline{H}$=C$\underline{H}$, OC$\underline{H}$Me), 4.25 (2 H, AB, J 17.7, ArC$\underline{H}_2$), 2.62–1.41 (10 H, m, 5 × CH$_2$), 1.39 (3 H, d, J 6.4, Me); δ_C (75 MHz; CDCl$_3$) 206.7, 170.0, 163.5, 156.1, 136.1, 135.2 (CH), 124.3 (CH), 114.6, 107.6, 103.5 (CH), 73.1 (CH), 46.7 (CH$_2$), 41.0 (CH$_2$), 37.6 (CH$_2$), 32.4 (CH$_2$), 25.2 (CH$_2$), 22.0 (CH$_2$), 18.8 (Me); m/z (CI) 355/353 (M$^+$, 25/72%), 335 (100).

(R)-1-Chloro-2,4-dihydroxy-7-methyl-7,8,9,12,13,14-hexahydro-6-oxa-16H-benzocyclotetradecene-5,15-dione 15e
mp 133°C −135°C; (Found: M$^+$, 352.1072. C$_{18}$H$_{21}^{35}$ClO$_5$ requires 352.1078); ν_{max} (KBr)/cm^{-1} 3361, 2930, 1715, 1651, 730; δ_H (300 MHz; CDCl$_3$) mixture of isomers 11.97 (1 H, s, OH), 11.86 (1 H, s, OH), 6.60 (1 H, s, ArH), 6.57 (1 H, s, ArH), 6.30 (1 H, s, OH), 5.49–5.02 (3 H, m, C$\underline{H}$=C$\underline{H}$, OC$\underline{H}$Me), 4.76–4.01 (2 H, m, ArC$\underline{H}_2$), 2.61–1.44 (10 H, m, 5 × CH$_2$) 1.39 (3 H, d, J 6.2, Me); δ_C (75 MHz; CDCl$_3$) mixture of isomers 205.8, 205.6, 170.5, 164.9, 163.7, 156.17, 156.12, 136.1, 135.6, 130.9 (CH), 130.7 (CH), 130.0 (CH), 128.4 (CH), 114.8, 107.2, 103.63 (CH), 163.60 (CH), 75.4 (CH), 74.3 (CH), 46.7 (CH$_2$), 46.6 (CH$_2$), 39.3 (CH$_2$), 37.6 (CH$_2$), 36.4 (CH$_2$), 33.9 (CH$_2$), 31.4 (CH$_2$), 28.8 (CH$_2$), 24.6 (CH$_2$), 23.4 (CH$_2$), 21.2 (CH$_2$), 20.4 (Me), 19.8 (Me), 19.4 (Me); m/z (EI) 354/352 (M$^+$, 4/12%), 284 (12), 183 (90), 55 (100).

(Z)-1-Chloro-2,4-dihydroxy-8,11,12,13-tetrahydro-7H,15H-6-oxabenzocyclotridecane-5,14-dione cis-15f
mp 164°C −166°C; (Found: MH$^+$, 325.0838. C$_{16}$H$_{17}$ClO$_5$ + H requires 325.0843); ν_{max} (KBr)/cm^{-1} 3333, 2923, 2854, 1693, 1667, 1313, 1231; δ_H (300 MHz; (CD$_3$)$_2$CO) 11.18 (1 H, s, OH), 9.77 (1 H, s, OH), 6.51 (1 H, s, ArH), 5.44–5.27 (2 H, m, C$\underline{H}$=C$\underline{H}$), 4.42 (2 H, s, OC$\underline{H}_2$), 4.08 (2 H, s, ArC$\underline{H}_2$), 2.47–2.36 (4 H, m, 2 × CH$_2$), 2.17–2.10 (2 H, m, CH$_2$), 1.70–1.62 (2 H, m, CH$_2$); δ_C (75 MHz; (CD$_3$)$_2$CO) 207.2, 172.4, 164.1, 159.9, 138.6 (C) 133.1 (CH), 130.0 (CH), 116.8, 109.3, 104.5 (CH), 67.3 (CH$_2$), 49.4 (CH$_2$), 39.4 (CH$_2$), 28.2 (CH$_2$), 26.0 (CH$_2$), 22.4 (CH$_2$); m/z (CI) 327/325 (MH$^+$, 34/100%), 307 (90), 286 (56), 263 (26).

(E)-1-Chloro-2,4-dihydroxy-8,11,12,13-tetrahydro-7H,15H-6-oxabenzocyclotridecane-5,14-dione trans-15f
mp 155°C −157°C; (Found: MH$^+$, 325.0832. C$_{16}$H$_{17}$ClO$_5$ + H requires 325.0843); ν_{max} (KBr)/cm^{-1} 3333, 2923, 2854, 1693, 1667, 1313, 1231; δ_H (300 MHz; (CD$_3$)$_2$CO) 11.41 (1 H, s, OH), 9.79 (1 H, s, OH), 6.67 (1 H, s, ArH), 5.56–5.32 (2 H, m, C$\underline{H}$=C$\underline{H}$), 4.60 (2 H, s, OC$\underline{H}_2$), 4.53 (2 H, s, ArC$\underline{H}_2$), 2.70–2.68 (2 H, m, CH$_2$), 2.50–2.40 (2 H, m, CH$_2$), 2.44–2.18 (2 H, m, CH$_2$), 2.08–1.92 (2 H, m, CH$_2$); δ_C (75 MHz; (CD$_3$)$_2$CO) 205.9, 172.4, 163.9, 159.6, 138.9 (C) 134.7 (CH), 129.1 (CH), 116.4, 109.6, 104.4 (CH), 66.1 (CH$_2$), 48.7 (CH$_2$), 42.7 (CH$_2$), 35.5 (CH$_2$), 34.0 (CH$_2$), 22.3 (CH$_2$); m/z (CI) 327/325 (MH$^+$, 34/100%), 307 (43), 291 (24), 263 (12).

1-Chloro-2,4-dihydroxy-7,8,11,12-tetrahydro-14H-6-oxabenzocyclododecene-5,13-dione 15g
mp 164°C −166°C; (Found: M$^+$, 310.0602. C$_{15}$H$_{15}^{35}$ClO$_5$ requires 310.0608); ν_{max} (KBr)/cm^{-1} 3232, 2927, 2852, 1696, 1654, 1315, 1241; δ_H (300 MHz; (CD$_3$)$_2$CO) mixture of isomers 11.78 (1 H, s, OH), 11.76 (1 H, s, OH), 9.73 (1 H, s, OH), 9.69 (1 H, s, OH), 6.52 (1 H, s, ArH), 5.71–5.29 (2 H, m, C$\underline{H}$=C$\underline{H}$), 4.48–4.25 (4 H, s, OC$\underline{H}_2$, ArC$\underline{H}_2$), 2.60–2.30 (4 H, m, 2 × CH$_2$); δ_C (75 MHz; (CD$_3$)$_2$CO) mixture of isomers 207.1, 205.7, 171.9, 163.9, 163.8, 158.7, 138.3 (C) 138.1, 132.0 (CH), 131.8 (CH), 130.0 (CH), 128.3 (CH), 115.8, 115.7, 107.8, 107.1, 103.6 (CH), 103.4 (CH), 66.6 (CH$_2$), 66.1 (CH$_2$), 50.7 (CH$_2$), 48.4 (CH$_2$), 42.9 (CH$_2$), 41.6 (CH$_2$), 32.2 (CH$_2$), 26.7 (CH$_2$), 25.0 (CH$_2$); m/z (EI) 312/310 (12/42%), 185/183 (44/100).

1-Chloro-2,4-dihydroxy-8,11,12,13,14,15-hexahydro-7H,17H-6-oxabenzocyclopentadecene-5,16-dione 15h

mp 129°C −131°C; (Found: MH$^+$, 353.1160. $C_{18}H_{21}{}^{35}ClO_5$ + H requires 353.1156); ν_{max} (KBr)/cm^{-1} 3272, 2935, 2860, 1688, 1238, 1115; δ_H (300 MHz; CDCl$_3$) δ_H (300 MHz; CDCl$_3$) *major isomer* 11.49 (1 H, s, OH), 6.57 (1 H, s, ArH), 6.36 (1 H, s, OH), 5.46–5.27 (2 H, m, C*H*=C*H*), 4.42 (2 H, t, J 4.52, OC*H*$_2$), 4.33 (2 H, s, ArC*H*$_2$), 2.54–2.48 (2 H, m, CH$_2$), 2.44–2.35 (2 H, m, CH$_2$), 2.07–2.01 (2 H, m, CH$_2$), 1.73–1.61 (2 H, m, CH$_2$), 1.44–1.24 (4 H, m, 2 × CH$_2$); *minor isomer* 11.59 (1 H, s, OH), 6.56 (1 H, s, ArH), 6.38 (1 H, s, OH), 4.47 (2 H, t, J 6.0, OC*H*$_2$); δ_C (75 MHz; CDCl$_3$) *mixture of isomers* 207.9, 170.9, 163.5, 156.6, 136.4 (C) 133.4 (CH), 127.8 (CH), 126.5 (CH), 114.7, 108.4, 104.0 (CH), 67.5 (CH$_2$), 66.5 (CH$_2$), 47.6 (CH$_2$), 41.9 (CH$_2$), 32.0 (CH$_2$), 30.6 (CH$_2$), 27.5 (CH$_2$), 27.1 (CH$_2$), 26.1 (CH$_2$), 25.8 (CH$_2$), 22.5 (CH$_2$), 21.9 (CH$_2$); *m/z* (CI) 355/353 (MH$^+$, 18/70%), 391 (53), 353 (75), 257 (100).

(R)-1-Chloro-2,4-dihydroxy-7-methyl-8,11,12,13,14,15-hexahydro-7H,17H-6-oxabenzocyclopentadecene-5,16-dione 15i

Colorless oil; (Found: MH$^+$, 367.1315. $C_{19}H_{23}{}^{35}ClO_5$ + H requires 367.1312); ν_{max}(KBr)/cm^{-1} 3522, 2934, 1712, 1656, 1602, 1308; δ_H (400 MHz; CDCl$_3$) *mixture of isomers* 6.59 (1 H, s, ArH), 6.43 (1 H, s, OH), 5.50–5.34 (3 H, m, C*H*=C*H*, OC*H*Me), 4.41 (2 H, s, ArC*H*$_2$), 2.67–2.59 (2 H, m, CH$_2$), 2.46–2.38 (2 H, m, CH$_2$), 2.33–1.45 (8 H, m, 4 × CH$_2$), 1.77 (3 H, d, J 6.3, Me), 1.45 (3 H, d, J 6.3, Me); δ_C (100 MHz; CDCl$_3$) *mixture of isomers* 207.5, 160.7, 163.0, 156.1, 136.2, 134.2 (CH), 124.4 (CH), 114.4, 107.9, 103.7 (CH), 73.2 (CH), 46.9 (CH$_2$), 40.9 (CH$_2$), 37.2 (CH$_2$), 29.7 (CH$_2$), 25.8 (CH$_2$), 25.2 (CH$_2$), 21.6 (CH$_2$), 18.8 (Me); *m/z* (ES) 391/389 ([M + Na]$^+$, 100/34%), 369/367 (MH$^+$, 30/10%), 349 (51).

1-Chloro-2,4-dihydroxy-7,8,11,12,13,14,15,16-octahydro-18H-6-oxabenzocyclohexadecene-5,17-dione 15j

mp 158°C −160°C; (Found: MH$^+$, 367.1290. $C_{19}H_{23}{}^{35}ClO_5$ + H requires 367.1312); ν_{max} (KBr)/cm^{-1} 3519, 2928, 2855, 1717, 1660, 1311; δ_H (400 MHz; CDCl$_3$) *mixture of isomers* 6.62 (1 H, s, ArH), 6.61 (1 H, s, ArH), 6.49 (1 H, s, OH), 6.23 (1 H, s, OH), 5.49–5.37 (2 H, m, C*H*=C*H*), 4.49–4.42 (4 H, s, OC*H*$_2$), 4.30 (2 H, s, ArC*H*$_2$), 2.59–2.46 (4 H, m, 2 × CH$_2$), 2.11–2.05 (2 H, m, CH$_2$), 1.72–1.64 (2 H, m, CH$_2$), 1.47–1.37 (4 H, m, 2 × CH$_2$), 1.27–1.19 (2 H, m, CH$_2$); δ_C (100 MHz; CDCl$_3$) *mixture of isomers* 206.0, 170.4, 163.5, 156.3, 136.1 (C) 133.3 (CH), 132.8 (CH), 127.0 (CH), 114.9, 107.3, 103.6 (CH), 68.4 (CH$_2$), 67.8 (CH$_2$), 47.0 (CH$_2$), 46.7 (CH$_2$), 39.7 (CH$_2$), 31.7 (CH$_2$), 29.9 (CH$_2$), 26.2 (CH$_2$), 25.7 (CH$_2$), 24.4 (CH$_2$), 21.9 (CH$_2$); *m/z* (CI) 369/367 (MH$^+$, 25/100%), 349 (22), 333 (16).

(E)-1-Chloro-9,10-epoxy-2,4-dihydroxy-7,8,11,12,13,14-hexahydro-6-oxa-16H-benzocyclotetradecene-5,15-dione 16a

Colorless oil; (Found: M$^+$, 354.0850. $C_{17}H_{19}{}^{35}ClO_6$ requires 354.0870); ν_{max} (film)/cm^{-1} 3370, 2927, 2856, 1713, 1658, 1237; δ_H (300 MHz; (CD$_3$)$_2$CO) 11.24 (1 H, s, OH), 9.68 (1 H, s, OH), 6.42 (1 H, s, ArH), 4.54–4.06 (4 H, m, 2 × CH$_2$), 2.78–0.65 (12 H, m, 5 × CH$_2$, 2 × CH); δ_C (75 MHz; CDCl$_3$) 206.9, 171.8, 163.7, 159.2, 138.0, 116.3, 108.5, 104.1 (CH), 64.1 (CH$_2$), 58.5 (CH), 57.6 (CH), 47.6 (CH$_2$), 41.2 (CH$_2$), 31.8 (CH$_2$), 31.7 (CH$_2$), 24.6 (CH$_2$), 23.8 (CH$_2$); *m/z* (FI) 356/354 (M$^+$, 35/100%), 268 (9).

1-Chloro-9,10-epoxy-2,4-dihydroxy-7-methyl-7,8,11,12,13,14-hexahydro-6-oxa-16H-benzocyclotetradecene-5,15-dione 16b

Colorless oil; (Found: M$^+$, 368.1000. $C_{18}H_{21}{}^{35}ClO_2$ requires 368.1027); ν_{max}(film)/cm^{-1} 3328, 2931, 1711, 1650, 1240, 731; δ_H (300 MHz; CDCl$_3$) *major isomer* 11.55 (1 H, s, OH), 6.64 (1 H, s, ArH), 6.17 (1 H, s, OH), 5.36–5.27 (1 H, m, OC*H*Me), 4.30 (2 H, AB, J 17.9, ArC*H*$_2$), 2.82–2.77 (1 H, m, C*H*(O)), 2.67–2.63 (1 H, m, C*H*(O)), 2.53–2.46 (2 H, m, CH$_2$), 2.33–1.23 (8 H, m, 4 × CH$_2$), 1.48 (3 H, 2 d, J 6.4, Me); *minor isomer* 11.34 (1 H, s, OH), 6.63 (1 H, s, ArH), 5.52–5.42 (1 H, m, OC*H*Me), 4.40 (2 H, AB, J 17.9, ArC*H*$_2$), 1.43 (3 H, 2 d, J 6.4, Me); δ_C (75 MHz; CDCl$_3$) *mixture of diastereoisomers* 205.8, 205.6, 169.1, 162.9, 155.6, 135.0, 114.2, 106.8, 103.2 (CH), 71.4 (CH), 70.8 (CH), 58.0 (CH$_2$), 56.8 (CH$_2$), 54.4 (CH$_2$), 54.2 (CH$_2$), 46.3 (CH$_2$), 46.0 (CH$_2$), 40.0 (CH$_2$), 39.5 (CH$_2$), 36.8 (CH$_2$), 35.7 (CH$_2$), 30.4 (CH$_2$), 28.9 (CH$_2$), 22.7 (CH$_2$), 22.1 (CH$_2$), 21.6 (CH$_2$), 21.3 (CH$_2$), 20.0 (Me), 18.4 (Me); *m/z* (FI) 370/368 (M$^+$, 41/100%), 290 (13), 202 (3).

1-Chloro-2,4-dihydroxy-7-methyl-7,8,9,10,11,12,13,14-octahydro-6-oxa-16H-benzocyclotetradecene-5,15-dione 17

mp 154°C −156°C; (Found: M$^+$, 354.1243. $C_{18}H_{23}{}^{35}ClO_5$ requires 354.1234); ν_{max} (KBr)/cm^{-1} 3437, 2931, 2835, 1703, 1645, 668; δ_H

(300 MHz; CDCl$_3$) 11.85 (1 H, s, OH), 6.73 (1 H, s, OH), 6.50 (1 H, s, ArH), 5.19–5.09 (1 H, m, OC*H*Me), 4.55 (2 H, AB, J 18.2, ArC*H*$_2$), 2.85–2.51 (2 H, m, CH$_2$), 1.95–0.87 (12 H, m, 6 × CH$_2$), 1.48 (3 H, d, J 6.0, Me); δ_C (75 MHz; CDCl$_3$) 207.1, 170.5, 163.5, 156.4, 135.6, 114.9, 107.2, 103.8 (CH), 74.5 (CH), 46.8 (CH$_2$), 39.7 (CH$_2$), 34.8 (CH$_2$), 26.4 (CH$_2$), 23.6 (CH$_2$), 23.2 (CH$_2$), 22.2 (CH$_2$), 21.8 (CH$_2$), 20.8 (Me); *m/z* (FI) 356/354 (M$^+$, 34/100%).

1,3-Dibromo-2,4-dihydroxy-8,11,12,13,14,15-hexahydro-7H,17H-6-oxabenzocyclopentadecene-5,16-dione 18

Colorless oil; (Found: MH$^+$, 474.9742. $C_{18}H_{20}{}^{79}Br_2O_5$ + H requires 474.9731); ν_{max} (CHCl$_3$)/cm^{-1} 3476, 2926, 2854, 1711, 1658, 1306; δ_H (400 MHz; CDCl$_3$) *mixture of isomers* 6.50 (1 H, s, OH), 5.51–5.40 (2 H, m, C*H*=C*H*), 4.54–4.42 (4 H, s, ArC*H*$_2$, COC*H*$_2$), 2.58–2.52 (2 H, m, CH$_2$), 2.46–2.42 (2 H, m, CH$_2$), 2.10–2.06 (2 H, m, CH$_2$), 1.74–1.27 (6 H, m, 3 × CH$_2$); δ_C (100 MHz; CDCl$_3$) *mixture of isomers* 206.4, 170.5, 159.7, 154.0, 137.2 (C) 133.1 (CH), 127.2 (CH), 108.8, 105.6, 98.3, 67.9 (CH$_2$), 66.8 (CH$_2$), 49.9 (CH$_2$), 49.6 (CH$_2$), 41.8 (CH$_2$), 41.7 (CH$_2$), 31.6 (CH$_2$), 30.1 (CH$_2$), 27.0 (CH$_2$), 26.7 (CH$_2$), 25.7 (CH$_2$), 25.6 (CH$_2$), 22.7 (CH$_2$), 21.5 (CH$_2$); *m/z* (CI) 474/476/478 (MH$^+$, 41/100/36%).

(R)-Pent-4-en-2-yl 3-chloro-4,6-dihydroxy-2-(2-oxo-oct-7-enyl)benzoate 19

Colorless oil; $[\alpha]_D^{23}$ − 26.0 (c 1.00, CHCl$_3$); (Found: M$^+$, 380.1389. $C_{20}H_{25}{}^{35}ClO_5$ requires 380.86); ν_{max} (film)/cm^{-1} 3262, 3077, 2933, 1652, 1433, 1244; δ_H (300 MHz; CDCl$_3$) 11.38 (1 H, s, OH), 6.54 (1 H, s, ArH) 6.44 (1 H, s, OH), 5.85–5.67 (2 H, m, 2 × C*H*=CH$_2$), 5.33–5.23 (1 H, m, OC*H*Me), 5.16–4.92 (4 H, m, 2 × CH=CH$_2$), 4.27 (2 H, AB, J 17.9, ArC*H*$_2$), 2.48 (2 H, t, J 7.3, CH$_2$), 2.42–2.33 (2 H, m, CH$_2$), 2.10–2.03 (2 H, m, CH$_2$), 1.69–1.61 (2 H, m, CH$_2$), 1.45–1.35 (2 H, m, CH$_2$), 1.30 (3 H, d, J 6.4, Me); δ_C (75 MHz; CDCl$_3$) 206.5, 169.2, 163.0, 156.2, 138.3 (CH), 135.7, 132.9 (CH), 118.6 (CH$_2$), 114.7 (CH$_2$), 107.5, 103.6 (CH) 72.6, 47.0 (CH$_2$), 41.8 (CH$_2$), 40.0 (CH$_2$), 33.5 (CH$_2$), 28.3 (CH$_2$), 23.0 (CH$_2$), 19.4 (Me); *m/z* (EI) 382/380 (M$^+$, 2/7%), 294 (10), 183 (100).

1-Chloro-2,4-dimethoxy-7-methyl-7,8,11,12,13,14-hexahydro-6-oxa-16H-benzocyclotetradecene-5,15-dione 25

Colorless oil; (Found: M$^+$, 380.1382. $C_{20}H_{25}{}^{35}ClO_5$ requires 380.1391); ν_{max} (film)/cm^{-1} 2936, 2846, 1721, 1592; δ_H (300 MHz; CDCl$_3$) 6.47 (1 H, s, ArH), 5.45–5.39 (2 H, m, C*H*=C*H*), 5.22–5.11 (1 H, m, OC*H*Me), 3.91 (3 H, s, Me), 3.84 (3 H, s, Me), 3.83 (2 H, AB, J 17.3, ArC*H*$_2$), 2.43–1.38 (10 H, m, 5 × CH$_2$), 1.36 (3 H, d, J 6.3, Me); δ_C (75 MHz; CDCl$_3$) 206.5, 167.0, 156.5, 156.4, 134.1 (CH), 132.7, 126.0 (CH), 118.5, 115.4, 95.5 (CH), 72.3 (CH), 56.2 (Me), 56.1 (Me), 45.1 (CH$_2$), 40.9 (CH$_2$), 38.8 (CH$_2$), 31.8 (CH$_2$), 25.9 (CH$_2$), 23.0 (CH$_2$), 20.0 (Me); *m/z* (FI) 382/380 (M$^+$, 35/100%), 366 (11), 346 (3).

1-Chloro-9,10-epoxy-2,4-dimethoxy-7-methyl-7,8,11,12,13,14-hexahydro-6-oxa-16H-benzocyclotetradecene-5,15-dione 26

Colorless oil; (Found: M$^+$, 396.1333. $C_{20}H_{25}{}^{35}ClO_6$ requires 396.1340); ν_{max} (film)/cm^{-1} 2932, 2850, 1714, 1604, 1261, 812; δ_H (300 MHz; CDCl$_3$) *mixture of diastereomers* 6.58–6.45 (1 H, m, ArH), 5.39–5.00 (2 H, m, CH$_2$), 4.24–3.56 (8 H, m, ArC*H*$_2$, 2 × CH$_2$), 2.78–1.17 (12 H, m, 5 × CH$_2$, 2 × CH), 1.36 (3 H, d, J 6.3, Me); δ_C (75 MHz; CDCl$_3$) *mixture of diastereomers* 206.2, 205.2, 166.2, 155.8, 155.3, 132,3, 131.3, 116.75, 114.5, 94.5 (CH), 69.7 (CH), 69.4 (CH), 60.68 (CH), 58.08 (CH), 57.5 (CH), 56.6 (CH), 55.4 (Me), 55.2 (Me), 55.1 (Me), 54.5 (CH), 43.6 (CH$_2$), 43.5 (CH$_2$), 40.5 (CH$_2$), 39.7 (CH$_2$), 37.8 (CH$_2$), 36.6 (CH$_2$), 29.6 (CH$_2$), 28.9 (CH$_2$), 28.6 (CH$_2$), 23.7 (CH$_2$), 22.9 (CH$_2$), 22.5 (CH$_2$), 21.6 (CH$_2$), 19.7 (Me), 18.8 (Me); *m/z* (FI) 398/396 (M$^+$, 23/100%).

Modeling

Molecular modeling was performed by using the Dock function in MOE (MOE 2004.03, Chemical Computing Group Inc., Cambridge, UK). In MOE-Dock, the configuration space includes all orientations and conformations of the ligand such that all of its atoms are inside the docking box.

Small-Molecule Crystallography

The atomic coordinates for compounds **14b**, **14f**, **15g**, and **23** have been deposited with the Cambridge Crystallographic Data Centre. The coordinates can be obtained upon request from The Director, Cambridge Crystallographic Data Centre, 12 Union Road, Cambridge, CB2 1EZ, United Kingdom.

Protein Crystallography

The expression, purification, and crystallization of the N-terminal domain of yeast Hsp90 have been previously described [62]. Cocrystallizations were conducted by dissolving the inhibitor in 100% DMSO at 50 mM and by adding 5 μl of this solution to 1 ml of the N-terminal domain of Hsp90 at 4 mg ml^{-1} in 20 mM Tris (pH 7.5) and 1 mM EDTA. The complex was then concentrated to 200 μl (20 mg ml^{-1}) and was crystallized as previously described [62]. Single crystals of approximate dimensions 0.3 × 0.2 × 0.2 mm appeared overnight. These were flash frozen after stepwise addition of glycerol to 30%, and data were collected on station ID23.1 and ID23.2 at the European Synchrotron Radiation Facility. The data were integrated by using MOSFLM and were scaled and merged with SCALA in CCP4.

The complex was initially solved by isomorphous replacement by using a previously determined N-terminal structure (PDB ID: 1AH6) in the usual space group, P4$_3$22. The model was refined in REFMAC5 in CCP4 and was rebuilt with COOT. The R$_{free}$ value did not refine below 30%; thus, other space groups were investigated. Refinement proceeded satisfactorily in C2, with four molecules in the asymmetric unit. The inhibitor library was built with SKETCHER. The inhibitor molecule and the waters were added in the final stages.

Biology

FP Assay

This is a measurement of binding competition with a fluorescent probe as described previously [33, 61].

Malachite Green Assay

A colorimetric assay for the release of inorganic phosphate upon hydrolysis of ATP was used to determine the potency of Hsp90 inhibitors against the enzyme. It is based on the formation of the phosphomolybdate complex and the subsequent reaction with malachite green [60].

Growth Inhibition Assay

The colorimetric sulforhodamine B assay (SRB) was used to measure growth inhibition as described previously [63]. The IC$_{50}$ was calculated as the drug concentration that inhibits cell growth by 50% compared with control growth.

Western Blotting

HCT116 cells were treated with 5 × IC$_{50}$ of selected compounds for 24 and 48 hr. Client proteins were immunoblotted and detected by enhanced chemiluminescence [63]. Antibody to Hsp70 was purchased from Stressgen Biotechnologies (Victoria, Canada); those for C-RAF, CDK4, and ERBB2 were purchased from Santa Cruz (CA, USA), and GAPDH was purchased from Chemicon (Hampshire, UK).

Isothermal Titration Calorimetry

Yeast Hsp90 was dialyzed against 20 mM Tris (pH 7.5) containing 1 mM EDTA and 5 mM NaCl; it was then diluted to 8 μM in the same buffer, but containing 2% DMSO. Compounds were dissolved in 100% DMSO at a concentration of 50 mM and were subsequently diluted to 100 μM in the same buffer as for Hsp90 (with 2% DMSO). Heats of the interaction were measured at 30°C on an MSC system (Microcal), with a cell volume of 1.458 ml. Ten aliquots of 27 μl of 100 μM compound were injected into 8 μM yeast Hsp90. Heats of dilution were determined in a separate experiment by injecting compound into buffer containing 2% DMSO, and the corrected data were fit with a nonlinear least square curve-fitting algorithm (Microcal Origin) with three floating variables: stoichiometry, binding constant, and change in enthalpy of interaction.

Supplemental Data

Supplemental Data include full experimental details and the characterization data for all intermediates and are available at http://www.chembiol.com/cgi/content/full/13/11/1203/DC1/.

References

1. Whitesell, L., and Lindquist, S. (2005). Hsp90 and the chaperoning of cancer. Nat. Rev. Cancer 5, 761–772.
2. Pearl, L.H., and Prodromou, C. (2006). Structure and mechanism of the Hsp90 molecular chaperone machinery. Annu. Rev. Biochem. 75, 271–294.
3. Maloney, A., and Workman, P. (2002). HSP90 as a new therapeutic target for cancer therapy: the story unfolds. Expert Opin. Biol. Ther. 2, 3–24.
4. Workman, P. (2004). Combinatorial attack on multistep oncogenesis by inhibiting the Hsp90 molecular chaperone. Cancer Lett. 206, 149–157.
5. Hanahan, D., and Weinberg, R.A. (2000). The hallmarks of cancer. Cell 100, 57–70.
6. Janin, Y.L. (2005). Heat shock protein 90 inhibitors. A text book example of medicinal chemistry. J. Med. Chem. 48, 7503–7512.
7. Chiosis, G., Lopes, E.C., and Solit, D. (2006). Heat shock protein-90 inhibitors: a chronicle from geldanamycin to today's agents. Curr. Opin. Investig. Drugs 7, 534–541.
8. Blagg, B.S.J., and Kerr, T.A. (2006). Hsp90 inhibitors: small molecules that transform the Hsp90 protein folding machinery into a catalyst for protein degradation. Med. Res. Rev. 26, 310–338.
9. McDonald, E., Workman, P., and Jones, K. (2006). Inhibitors of the Hsp90 molecular chaperone: attacking the master regulator in cancer. Curr. Top. Med. Chem. 6, 1091–1107.
10. Sharp, S., and Workman, P. (2006). Inhibitors of the Hsp90 molecular chaperone: current status. Adv. Cancer Res. 95, 323–348.
11. Gallo, K.A. (2006). Targeting HSP90 to halt neurodegeneration. Chem. Biol. 13, 115–116.
12. Prodromou, C., Roe, S.M., O'Brien, R., Ladbury, J.E., Piper, P.W., and Pearl, L.H. (1997). Identification and structural characterization of the ATP/ADP-binding site in the Hsp90 molecular chaperone. Cell 90, 65–75.
13. Ali, M.M.U., Roe, S.M., Vaughan, C.K., Meyer, P., Panaretou, B., Piper, P.W., Prodromou, C., and Pearl, L.H. (2006). Crystal structure of an Hsp90-nucleotide-p23/Sba1 closed chaperone complex. Nature 440, 1013–1017.
14. Schulte, T.W., An, W.G., and Neckers, L.M. (1997). Geldanamycin-induced destabilization of Raf-1 involves the proteasome. Biochem. Biophys. Res. Commun. 239, 655–659.
15. Roe, S.M., Prodromou, C., O'Brien, R., Ladbury, J.E., Piper, P.W., and Pearl, L.H. (1999). Structural basis for inhibition of the Hsp90 molecular chaperone by the antitumor antibiotics radicicol and geldanamycin. J. Med. Chem. 42, 260–266.
16. Chiosis, G., Vilenchik, M., Kim, J., and Solit, D. (2004). Hsp90: the vulnerable chaperone. Drug Discov. Today 9, 881–888.
17. Marcu, M.G., Chadli, A., Bouhouche, I., Catelli, M., and Neckers, L.M. (2000). The heat shock protein 90 antagonist novobiocin interacts with a previously unrecognized ATP-binding domain in the carboxyl terminus of the chaperone. J. Biol. Chem. 275, 37181–37186.
18. Yu, X.M., Shen, G., Neckers, L., Blake, H., Holzbeierlein, J., Cronk, B., and Blagg, B.S.J. (2005). Hsp90 inhibitors identified from a library of novobiocin analogues. J. Am. Chem. Soc. 127, 12778–12779.
19. Allan, R.K., Mok, D., Ward, B.K., and Ratajczak, T. (2006). Modulation of chaperone function and cochaperone interaction by novobiocin in the C-terminal domain of Hsp90: evidence that coumarin antibiotics disrupt Hsp90 dimerization. J. Biol. Chem. 281, 7161–7171.
20. Dehner, A., Furrer, J., Richter, K., Schuster, I., Buchner, J., and Kessler, H. (2003). NMR chemical shift perturbation study of the N-terminal domain of Hsp90 upon binding of ADR AMP-PNP, geldanamycin, and radicicol. ChemBioChem 4, 870–877.

21. Banerji, U., O'Donnell, A., Scurr, M., Pacey, S., Stapleton, S., Asad, Y., Simmons, L., Maloney, A., Raynaud, F., Campbell, M., et al. (2005). Phase I pharmacokinetic and pharmacodynamic study of 17-allylamino, 17-demethoxygeldanamycin in patients with advanced malignancies. J. Clin. Oncol. 23, 4152–4161.

22. Pacey, S., Banerji, U., Judson, I., and Workman, P. (2006). Hsp90 inhibitors in the clinic. Handb. Exp. Pharmacol. 172, 331–358.

23. Chiosis, G., Timaul, M.N., Lucas, B., Munster, P.N., Zheng, F.F., Sepp-Lorenzino, L., and Rosen, N. (2001). A small molecule designed to bind to the adenine nucleotide pocket of Hsp90 causes Her2 degradation and the growth arrest and differentiation of breast cancer cells. Chem. Biol. 8, 289–299.

24. Wright, L., Barril, X., Dymock, B., Sheridan, L., Surgenor, A., Beswick, M., Drysdale, M., Collier, A., Massey, A., Davies, N., et al. (2004). Structure-activity relationships in purine-based inhibitor binding to HSP90 isoforms. Chem. Biol. 11, 775–785.

25. Vilenchik, M., Solit, D., Basso, A., Huezo, H., Lucas, B., He, H.Z., Rosen, N., Spampinato, C., Modrich, P., and Chiosis, G. (2004). Targeting wide-range oncogenic transformation via PU24FCl, a specific inhibitor of tumor Hsp90. Chem. Biol. 11, 787–797.

26. Llauger, L., He, H.Z., Kim, J., Aguirre, J., Rosen, N., Peters, U., Davies, P., and Chiosis, G. (2005). Evaluation of 8-arylsulfanyl, 8-arylsulfoxyl, and 8- arylsulfonyl adenine derivatives as inhibitors of the heat shock protein 90. J. Med. Chem. 48, 2892–2905.

27. He, H.Z., Zatorska, D., Kim, J., Aguirre, J., Llauger, L., She, Y.H., Wu, N., Immormino, R.M., Gewirth, D.T., and Chiosis, G. (2006). Identification of potent water soluble purine-scaffold inhibitors of the heat shock protein 90. J. Med. Chem. 49, 381–390.

28. Biamonte, M.A., Shi, J.D., Hong, K., Hurst, D.C., Zhang, L., Fan, J.H., Busch, D.J., Karjian, P.L., Maldonado, A.A., Sensintaffar, J.L., et al. (2006). Orally active purine-based inhibitors of the heat shock protein 90. J. Med. Chem. 49, 817–828.

29. McDonald, E., Jones, K., Brough, P.A., Drysdale, M.J., and Workman, P. (2006). Discovery and development of pyrazole-scaffold Hsp90 inhibitors. Curr. Top. Med. Chem. 6, 1193–1203.

30. Cheung, K.M.J., Matthews, T.P., James, K., Rowlands, M.G., Boxall, K.J., Sharp, S.Y., Maloney, A., Roe, S.M., Prodromou, C., Pearl, L.H., et al. (2005). The identification, synthesis, protein crystal structure and in vitro biochemical evaluation of a new 3,4-diarylpyrazole class of Hsp90 inhibitors. Bioorg. Med. Chem. Lett. 15, 3338–3343.

31. Barril, X., Beswick, M.C., Collier, A., Drysdale, M.J., Dymock, B.W., Fink, A., Grant, K., Howes, R., Jordan, A.M., Massey, A., et al. (2006). 4-Amino derivatives of the Hsp90 inhibitor CCT018159. Bioorg. Med. Chem. Lett. 16, 2543–2548.

32. Kreusch, A., Han, S.L., Brinker, A., Zhou, V., Choi, H.S., He, Y., Lesley, S.A., Caldwell, J., and Gu, X.J. (2005). Crystal structures of human HSP90α-complexed with dihydroxyphenylpyrazoles. Bioorg. Med. Chem. Lett. 15, 1475–1478.

33. Dymock, B.W., Barril, X., Brough, P.A., Cansfield, J.E., Massey, A., McDonald, E., Hubbard, R.E., Surgenor, A., Roughley, S.D., Webb, P., et al. (2005). Novel, potent small-molecule inhibitors of the molecular chaperone Hsp90 discovered through structure-based design. J. Med. Chem. 48, 4212–4215.

34. Brough, P.A., Barril, X., Beswick, M., Dymock, B.W., Drysdale, M.J., Wright, L., Grant, K., Massey, A., Surgenor, A., and Workman, P. (2005). 3-(5-Chloro-2,4-dihydroxyphenyl)pyrazole-4-carboxamides as inhibitors of the Hsp90 molecular chaperone. Bioorg. Med. Chem. Lett. 15, 5197–5201.

35. Barril, X., Brough, P., Drysdale, M., Hubbard, R.E., Massey, A., Surgenor, A., and Wright, L. (2005). Structure-based discovery of a new class of Hsp90 inhibitors. Bioorg. Med. Chem. Lett. 15, 5187–5191.

36. Delmotte, P., and Delmotteplaquee, J. (1953). A new antifungal substance of fungal origin. Nature 171, 344.

37. Mirrington, R.N., Ritchie, E., Shoppee, C.W., Taylor, W.C., and Sternhell, S. (1964). The constitution of radicicol. Tetrahedron Lett. 7, 365–370.

38. Turbyville, T.J., Wijeratne, E.M.K., Liu, M.X., Burns, A.M., Seliga, C.J., Luevano, L.A., David, C.L., Faeth, S.H., Whitesell, L., and Gunatilaka, A.A.L. (2006). Search for Hsp90 inhibitors with potential anticancer activity: isolation and SAR studies of radicicol and monocillin I from two plant-associated fungi of the Sonoran Desert. J. Nat. Prod. 69, 178–184.

39. Sharma, S.V., Agatsuma, T., and Nakano, H. (1998). Targeting of the protein chaperone, HSP90, by the transformation suppressing agent, radicicol. Oncogene 16, 2639–2645.

40. Soga, S., Neckers, L.M., Schulte, T.W., Shiotsu, Y., Akasaka, K., Narumi, H., Agatsuma, T., Ikuina, Y., Murakata, C., Tamaoki, T., et al. (1999). KF25706, a novel oxime derivative of radicicol, exhibits in vivo antitumor activity via selective depletion of Hsp90 binding signaling molecules. Cancer Res. 59, 2931–2938.

41. Soga, S., Shiotsu, Y., Akinaga, S., and Sharma, S.V. (2003). Development of radicicol analogues. Curr. Cancer Drug Targets 3, 359–369.

42. Agatsuma, T., Ogawa, H., Akasaka, K., Asai, A., Yamashita, Y., Mizukami, T., Akinaga, S., and Saitoh, Y. (2002). Halohydrin and oxime derivatives of radicicol: synthesis and antitumor activities. Bioorg. Med. Chem. 10, 3445–3454.

43. Lampilas, M., and Lett, R. (1992). Convergent stereospecific total synthesis of monochiral monocillin-I related macrolides. Tetrahedron Lett. 33, 773–776.

44. Lampilas, M., and Lett, R. (1992). Convergent stereospecific total synthesis of monocillin-I and monorden (or radicicol). Tetrahedron Lett. 33, 777–780.

45. Tichkowsky, I., and Lett, R. (2002). Convergent stereospecific total synthesis of monocillin I and radicicol: some simplifications and improvements. Tetrahedron Lett. 43, 3997–4001.

46. Tichkowsky, I., and Lett, R. (2002). Improvements of the total synthesis of monocillin I and radicicol via Miyaura-Suzuki couplings. Tetrahedron Lett. 43, 4003–4007.

47. Garbaccio, R.M., Stachel, S.J., Baeschlin, D.K., and Danishefsky, S.J. (2001). Concise asymmetric syntheses of radicicol and monocillin I. J. Am. Chem. Soc. 123, 10903–10908.

48. Barluenga, S., Moulin, E., Lopez, P., and Winssinger, N. (2005). Solution- and solid-phase synthesis of radicicol (monorden) and pochonin C. Chemistry 11, 4935–4952.

49. Yamamoto, K., Garbaccio, R.M., Stachel, S.J., Solit, D.B., Chiosis, G., Rosen, N., and Danishefsky, S.J. (2003). Total synthesis as a resource in the discovery of potentially valuable antitumor agents: cycloproparadicicol. Angew. Chem. Int. Ed. Engl. 42, 1280–1284.

50. Yang, Z.Q., Geng, X.D., Solit, D., Pratilas, C.A., Rosen, N., and Danishefsky, S.J. (2004). New efficient synthesis of resorcinylic macrolides via ynolides: establishment of cycloproparadicicol as synthetically feasible preclinical anticancer agent based on Hsp90 as the target. J. Am. Chem. Soc. 126, 7881–7889.

51. Geng, X.D., Yang, Z.Q., and Danishefsky, S.J. (2004). Synthetic development of radicicol and cycloproparadicicol: highly promising anticancer agents targeting hsp90. Synlett 1325–1333.

52. Clevenger, R.C., and Blagg, B.S.J. (2004). Design, synthesis, and evaluation of a radicicol and geldanamycin chimera, radamide. Org. Lett. 6, 4459–4462.

53. Shen, G., and Blagg, B.S.J. (2005). Radester, a novel inhibitor of the Hsp90 protein folding machinery. Org. Lett. 7, 2157–2160.

54. Wang, M.W., Shen, G., and Blagg, B.S.J. (2006). Radanamycin, a macrocyclic chimera of radicicol and geldanamycin. Bioorg. Med. Chem. Lett. 16, 2459–2462.

55. Moulin, E., Zoete, V., Barluenga, S., Karplus, M., and Winssinger, N. (2005). Design, synthesis, and biological evaluation of HSP90 inhibitors based on conformational analysis of radicicol and its analogues. J. Am. Chem. Soc. 127, 6999–7004.

56. Atrash, B., Cooper, T.S., Sheldrake, P., Workman, P., and McDonald, E. (2006). Development of synthetic routes to macrocyclic compounds based on the HSP90 inhibitor radicicol. Tetrahedron Lett. 47, 2237–2240.

57. Cooper, T.S., Atrash, B., Sheldrake, P., Workman, P., and McDonald, E. (2006). Synthesis of resorcinylic macrocycles related to radicicol via ring-closing metathesis. Tetrahedron Lett. 47, 2241–2243.

58. Barluenga, S., Lopez, P., Moulin, E., and Winssinger, N. (2004). Modular asymmetric synthesis of pochonin C. Angew. Chem. Int. Ed. Engl. 43, 3467–3470.

59. Stork, G., and Zhao, K. (1989). A simple method of dethioacetalization. Tetrahedron Lett. 30, 287–290.

60. Rowlands, M.G., Newbatt, Y.M., Prodromou, C., Pearl, L.H., Workman, P., and Aherne, W. (2004). High-throughput screening assay for inhibitors of heat-shock protein 90 ATPase activity. Anal. Biochem. *327*, 176–183.

61. Howes, R., Barril, X., Dymock, B.W., Grant, K., Northfield, C.J., Robertson, A.G.S., Surgenor, A., Wayne, J., Wright, L., James, K., et al. (2006). A fluorescence polarization assay for inhibitors of Hsp90. Anal. Biochem. *350*, 202–213.

62. Prodromou, C., Piper, P.W., and Pearl, L.H. (1996). Expression and crystallization of the yeast Hsp82 chaperone, and preliminary X-ray diffraction studies of the amino-terminal domain. Proteins *25*, 517–522.

63. Sharp, S.Y., Kelland, L.R., Valenti, M.R., Brunton, L.A., Hobbs, S., and Workman, P. (2000). Establishment of an isogenic human colon tumor model for NQO1 gene expression: application to investigate the role of DT-diaphorase in bioreductive drug activation in vitro and in vivo. Mol. Pharmacol. *58*, 1146–1155.

64. Fletcher, D.A., McMeeking, R.F., and Parkin, D.J. (1996). The United Kingdom Chemical Database Service. J. Chem. Inf. Comp. Sci. *36*, 746–749.

Accession Numbers

Coordinates for protein-bound structures of **15a**, **15f** *cis*, **15f** *trans*, and **15h** have been deposited in the Protein Data Bank with codes 2CGF, 2IWS, 2IWU, and 2IWX, respectively.